Ethanol hypersensitivity and olfactory discrimination defect in mice lacking a homolog of *Drosophila neuralized*

Youlin Ruan*, Laurence Tecott†, Ming-Ming Jiang*, Lily Yeh Jan*, and Yuh Nung Jan*‡

*Departments of Physiology and Biochemistry, Howard Hughes Medical Institute, and †Department of Psychiatry and Center for Neurobiology and Psychiatry, University of California, San Francisco, CA 94143

Contributed by Yuh Nung Jan, June 25, 2001

Neurogenic genes in the Notch receptor-mediated signaling pathway play important roles in neuronal cell fate specification as well as neuronal differentiation. The *Drosophila neuralized* gene is one of the neurogenic genes. We have cloned a mouse homolog of *Drosophila neuralized*, *m*-neu1, and found that the *m*-neu1 transcript is expressed in differentiated neurons. Mice deficient for *m*-neu1 are viable and morphologically normal, but exhibit specific defects in olfactory discrimination and hypersensitivity to ethanol. These findings reveal an essential role of *m*-neu1 in ensuring proper processing of certain information in the adult brain.

Many molecular mechanisms controlling neural development and neural function are evolutionarily conserved (1–3). One example is the *Notch*-mediated cell–cell interaction, a mechanism to mediate signaling between adjacent cells and thereby to specify cell fates in organisms ranging from worms and flies to mammals (4). In a given organism, the *Notch* signaling mechanism functions in many developmental processes as well as in adult life (5, 6). In the nervous system, the *Notch* signaling mechanism is involved in neurogenesis (1, 3), neuronal differentiation (2, 6), axon path finding (7, 8), and neurite growth (9, 10). The importance of *Notch* in maintaining normal neuronal function in the adult has been revealed by a number of human neurological syndromes because of defects in *Notch* signaling (6).

Like *Notch*, the *Drosophila neuralized* gene (*neu*) is a neurogenic gene whose function is to limit the number of neuronal precursor cells and to specify sensory organ as well as R8 photoreceptor cell fates (11–17). Genetic analyses suggest that *neuralized* interacts with other neurogenic genes, such as the *Notch* receptor and the *Delta* ligand for cell–cell interaction (18). Recent studies (15–17) revealed that *neuralized* functions cell-autonomously to regulate a subset of *Notch*-dependent processes. How *neuralized* affects *Notch* signaling is unknown at present. An interesting possibility is that Neu protein with its C3HC4 RING finger domain functions as an E3 ubiquitin ligase to modulate *Notch* signaling (15–17, 19).

We have cloned a mouse homolog of *Drosophila neuralized*, *m*-neu1, and found that it is expressed in differentiated neurons. We examined its functional role in the nervous system by generating a loss-of-function allele of *m*-neu1. Whereas the *m*-neu1 null mutants exhibit normal performance in a number of behavioral tests, including Morris water maze assay for learning and memory, they display specific functional lesions in olfactory discrimination and ethanol effects on motor coordination. These studies identify specific functions of the adult brain that are critically dependent on *m*-neu1 activity.

Materials and Methods

Isolation of a Mouse *Neuralized* Homolog. A mouse midgestation embryonic cDNA library (Stratagene) was screened with fragments of *Drosophila neuralized* cDNA as probes. In brief, the duplicated nylon filters containing mouse phage cDNAs were prehybridized at 55°C overnight in Church buffer (20): 1% BSA/1 mM EDTA/0.5 M Na_2HPO_4, pH 7.2/7% SDS. Hybridization was performed at 55°C for 24 h in the Church buffer containing $\approx 10^6$ cpm/ml of ^{32}P-labeled probe. Low stringency washes were conducted in 2 × SSC, 0.1% SDS at room temperature (2 × 15 min) followed by in 2 × SSC, 0.1% SDS at 40°C (2 × 30 min).

Northern Blot Analysis and Reverse Transcription (RT)-PCR. Northern blot hybridization was performed with a ^{32}P-labeled, randomly primed, 0.6-kb *m*-neu1 fragment (from the 5′-end of *m*-neu1 cDNA) or an *actin* probe to ensure equal RNA loading. For RT-PCR, total RNA was isolated from a series of embryonic stages of mouse embryos, from E7.5 to E17.5. Oligo(dT)-primed reverse transcription was performed on 2.0 μg of total RNA from each embryonic stage with mouse-murine leukemia virus reverse transcriptase (GIBCO/BRL). An equal amount (1/20) of cDNA product from each reaction served as a template for PCR amplification. The PCR amplification was performed by using primers specific to *m*-neu1: 5′-AGTGATGAATGCACCATTTGCTATG-3′ (a sense primer) and 5′-GAGGAAGAGTTTGCAAACTGTAGAA-3′ (an antisense primer). The cycling parameters used were as follows: 94°C for 1 min, 60°C for 2 min, and 72°C for 1 min for 30 cycles. Equal loading was ensured by PCR amplification using mouse *actin* primers: 5′-CACACCTTCTACAATGAGCTGCGTGT-3′ (a sense primer) and 5′-GGTGAGGATCTTCATGAGGTAGTC-3′ (an antisense primer).

Generation and Genotyping of Knockout Mice. *m*-neu1 cDNA was used to screen a 129/Sv mouse genomic library (Stratagene). Genomic DNA fragments were used to create a targeting construct in which the last three coding exons of *m*-neu1 were replaced by the pGK-neo selectable marker. pBS-tk was placed at one end of the genomic fragment for use in a positive–negative selection scheme. In brief, a 5.6-kb *Eco*RV–*Not*I fragment was used as a 5′ arm, and a 2.2-kb *Xho*I–*Xho*I fragment was used as a 3′ arm. This targeting vector was linearized with *Not*I and electroporated into JM1 embryonic stem (ES) cells. After a 24-h growth period in nonselective medium and an 8-day growth period in selective medium (300 μg/ml G418 and 0.2 μM FIAU), individual doubly resistant colonies were picked. ES cell clones (192 total) were screened for targeting event by genomic Southern hybridization analysis. After digestion with *Bam*HI, blots were hybridized with a 5′ external probe. Twelve clones tested positive for homologous recombination at 5′ arm region were

NEUROBIOLOGY

Abbreviations: *m*-neu1, mouse *neuralized 1*; *d-neu*, *Drosophila neuralized*; ES, embryonic stem; RT, reverse transcription.

Data deposition: The sequence reported in this paper has been deposited in the GenBank database (accession no. AF400063).

‡To whom reprint requests should be addressed. E-mail: ynjan@itsa.ucsf.edu.

The publication costs of this article were defrayed in part by page charge payment. This article must therefore be hereby marked "*advertisement*" in accordance with 18 U.S.C. §1734 solely to indicate this fact.

confirmed by *Eco*RV digestion followed by hybridization using a 3′ external probe. Three clones were microinjected into C57BL/6 mouse blastocysts, and the resulting chimeras mated to C57BL/6 mice. Germ-line transmission was obtained from all three injected ES clones.

Genotyping of mutant mice was carried out by using Southern blot or PCR (primer 1, 5′-GATTGGGCTGAAAGAGTTTC-AGGCA-3′; primer 2, 5′-GCTACATGTCTGCTAACTCTCT-CCA-3′; primer 3, 5′-CATAGCGTTGGCTACCCGTGAT-ATT-3′). As shown in Fig. 4*c*, primer 1 and primer 2 generate a 0.19-kb fragment that represents wild-type allele, whereas primer 2 and primer 3 produce a 0.27-kb fragment indicative of the knockout allele.

Histology, *in Situ* Hybridization, and Immunohistochemistry. For histological analysis, mice were anesthetized and fixed by perfusion with 4% paraformaldehyde in 0.1 M phosphate buffer. Brains were dehydrated in ethanol, embedded in paraffin, and serially sectioned at 5 μm. Sections were used for conventional staining. For *in situ* hybridization, digoxigenin-labeled sense and antisense riboprobes were produced with a digoxigenin RNA labeling kit (Boehringer Mannheim) according to the manufacturer's instructions. Whole mount *in situ* hybridization was performed essentially as described (21). Tissue section *in situ* hybridization was processed as described (22). For BrdUrd-labeling experiments, BrdUrd (Sigma) was injected intraperitoneally (50 mg/kg). Brain sections were treated with 2 N HCl for 30 min at 37°C and rinsed several times with PBS before adding mouse anti-BrdUrd (Novocastra).

Olfactory Discrimination. Olfactory discrimination was performed as previously described (23–25). Male mice (≈3 months) were housed individually without water but with a restricted fluid access to the saccharin–phthalic acid solution (2.1×10^{-2} M sodium saccharin and 10^{-3} M phthalic acid) for 1 h each day for 7 days to ensure that they would commence drinking when the tube was placed. On day 8, each mouse was given access to a saccharin–phthalic solution containing a 10^{-3} dilution of isovaleric acid for 10 min. Immediately after this exposure, each mouse was removed from its cage, injected intraperitoneally with 15 μl/g body weight of 0.6 M LiCl to induce an aversive state, and then returned to a clean cage. Twenty-four hours later, each mouse was provided two bottles, one with the control saccharin–phthalic acid solution and the other with the same solution plus isovaleric acid. For every 24 h, the amount of fluid consumed was determined by weighing each bottle, and the positions of the bottles in the cage were reversed. Every 48 h, the odorant concentration was reduced and the experiment continued. A preference percentage was calculated as the amount of isovaleric acid solution consumed divided by the total amount of liquid consumed for each mouse over the 48-h test period.

Water Maze Task. Male mice (≈3 months) were subjected to the Morris water maze test for spatial learning and memory. A training trial involved placing a mouse in the pool at a start site in one of the four quadrants, chosen randomly for each trial, and allowing the mouse to search for the platform. The time required for the mouse to climb onto the platform was recorded. The mice were trained with eight trials (two blocks) per day for 7 consecutive days. For day 1 and day 2, mice were trained with a visible-platform task. From day 3 to day 7, mice were trained with a hidden-platform task. In the probe test, which is just after the 7-day training, the mouse was allowed to search for 60 s in the absence of platform. Recordings of the probe trial were viewed to determine the time spent in each quadrant.

Ethanol Effect on Motor Coordination. Male mice (≈3 months) were initially allowed to acclimate to a rotarod before testing. The acclimation period consisted of placing each mouse on the stationary rotarod, which was then accelerated from 0 to 8 rpm over a 10-s period. Performance on the task was assessed by the latency until the mouse fell off the device. Latency to fall was recorded automatically. Ethanol was diluted to 20% (vol/vol) in saline. Mice were injected intraperitoneally with saline or 2.0 g/kg ethanol and tested on the rotarod 30 min after injection. Latencies for mice that stayed on the rotarod for >150 s were recorded as 150 s.

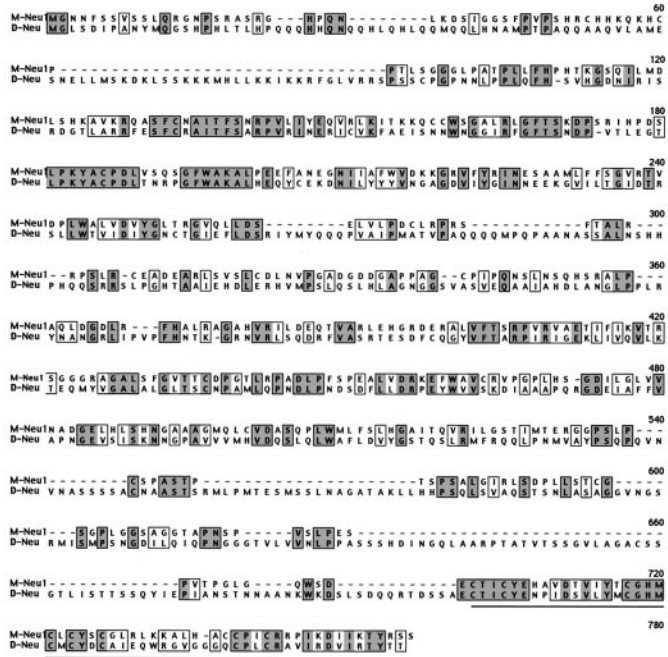

Fig. 1. The predicted amino acid sequence of M-Neu1 and sequence alignment of M-Neu1 and D-Neu. The first methionine of M-Neu1 was selected based on Kozak's rule and identification of an in-frame upstream termination codon. The amino acid sequences of M-Neu1 and D-Neu were aligned by using the CLUSTAL W sequence alignment program. Identical residues are outlined and shaded, and similar residues are outlined. – represents gap in the sequence. The sequences of the C3HC4 RING zinc finger domain are underlined.

Results

Isolation of *m*-neu1. To isolate mouse homolog(s) of *Drosophila neuralized* (*d-neu*), we used a cloning strategy of low-stringency hybridization screening, using *d-neu* cDNA to isolate a full-length *m*-neu1 from a mouse embryonic cDNA library. Sequence analysis of *m*-neu1 revealed an ORF encoding a predicted protein of 574 aa (Fig. 1). M-Neu1 and D-Neu display extensive similarity throughout the protein (Fig. 1), including a C-terminal C3HC4 RING zinc finger domain (amino acids 521–560, 55% identity). The RING zinc finger domain represents a small protein module that uses zinc ions for stability (26). It is found in a wide variety of functionally distinct proteins and may act as a novel protein-interaction module. Evolutionary conservation of the C-terminal C3HC4 RING zinc finger domain is underscored by the sequences of one *Caenorhabditis elegans neuralized* homolog (C-Neu) in database, which bears a similar extent of homology to M-Neu1 as does D-Neu, and a human homolog of *Drosophila neuralized* reported recently (27), which is 94% identical to M-Neu1 at the amino acid level. These data suggest that *neuralized* is an evolutionarily conserved molecule.

***m*-neu1 Expression.** The embryonic and adult expression of *m*-neu1 was examined by Northern blot and RT-PCR. A 4.3-kb

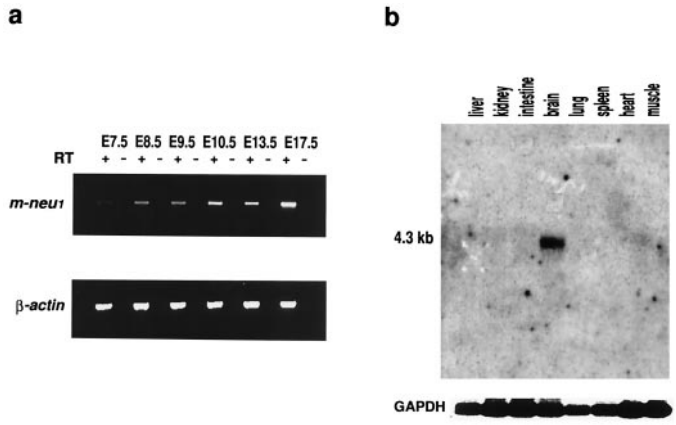

Fig. 2. Tissue distribution and expression profile of *m*-neu1 mRNA. (*a*) RT-PCR analysis of *m*-neu1 expression during mouse embryogenesis. Whole embryos were isolated from embryonic day 7.5 (E7.5) to embryonic day 17.5 (E17.5) and used to prepare total RNA. An equivalent amount of total RNA was transcribed and subjected to PCR. RNAs treated without reverse transcriptase (RT−) were used as negative controls. (*b*) Northern blot analysis of *m*-neu1 expression in adult mouse organs. Two micrograms of poly(A)$^+$ RNA was used in each lane. A probe against glyceraldehyde-3-phosphate dehydrogenase (GAPDH) was used as a control.

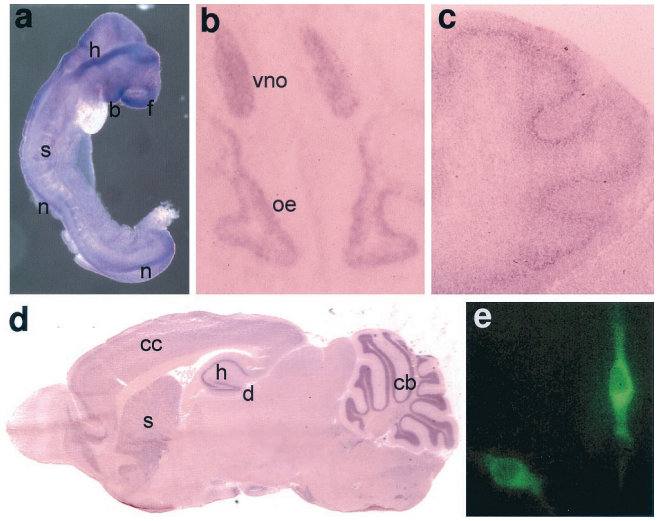

Fig. 3. *m*-neu1 expression in embryonic, postnatal, and adult mice. Whole embryos or sections were hybridized with an antisense RNA probe for *m*-neu1. (*a*) *m*-neu1 expression in an E8.5 embryo. High levels of *m*-neu1 expression in E8.5 embryo are observed in the forebrain neural fold (f), the hindbrain neural fold (h), the first branchial arch (b), the neural tube (n), and the somites (s). (*b*) *m*-neu1 expression in E13.5 olfactory epithelium (oe) and vomeronasal organ (vno). (*c*) *m*-neu1 expression in P0 cerebellum. (*d*) *m*-neu1 expression in adult brain. High levels of *m*-neu1 expression in adult brain are observed in the cerebral cortex (cc), cerebellum (cb), striatum (s), hippocampus (h), and dentate gyrus (d). (e) Cytoplasmic localization of M-Neu1/GFP fusion protein. A construct of the *m*-neu1 gene fused to the gene encoded the green fluorescence protein was transfected into cultured mouse neuroblastoma Neuro2a cells (America Type Culture Collection). The expressed fusion protein is primarily in the cytoplasm.

m-neu1 transcript was detected (Fig. 2*b*). The *m*-neu1 transcript is expressed from embryo to adult, similar to *d-neu*. Whereas low levels of *m*-neu1 mRNA could be detected at embryonic day 7.5 (E7.5), higher levels of *m*-neu1 mRNA were detected later in embryogenesis (Fig. 2*a*). In the adult, the expression of *m*-neu1 appeared to be highly restricted to the brain and was undetectable in other tissues including heart, liver, kidney, intestine, lung, spleen, and skeletal muscle (Fig. 2*b*).

To gain insight into the potential function of *m*-neu1, we analyzed the spatial distribution of *m*-neu1 transcript by *in situ* hybridization. At E8.5 (embryo with 11–13 pairs of somites), *m*-neu1 is mainly expressed in the nervous system, although it is also expressed in somites and the first branchial arch (Fig. 3*a*). The *m*-neu1 transcript was detected throughout the neural tube along the rostral-caudal neural axis. In the brain, *m*-neu1 is highly expressed in the forebrain neural fold and the hindbrain neural fold (Fig. 3*a*). Later during embryogenesis, the *m*-neu1 transcript was detected in differentiated neurons in the brain and the spinal cord, as well as in sensory neurons of the olfactory epithelium and the vomeronasal organ (Fig. 3*b* and data not shown). At postnatal stage, the *m*-neu1 transcript was also detected in the nervous system (Fig. 3*c* and data not shown). In the adult brain, the *m*-neu1 transcript is expressed in several regions with high expression in the cerebral cortex, cerebellum, striatum, hippocampus, and dentate gyrus (Fig. 3*d*). When expressed in cultured mouse neuroblastoma Neuro2a cells, a fusion protein of the *m*-neu1 gene product and the green fluorescence protein (GFP) is primarily in the cytoplasm (Fig. 3*e*).

Generation of Mice with a Disrupted *m*-neu1 Gene. To examine the *in vivo* function of *m*-neu1, we disrupted the *m*-neu1 gene by homologous recombination in mouse ES cells. An isogenic targeting construct was made to delete the last three exons, which encode 61% of the protein, by replacing a 4.8-kb genomic fragment with the neomycin resistance gene (Fig. 4*a*). JM1 ES cells were electroporated with the linearized targeting construct and selected in G418 and FIAU (28, 29). Double-resistant clones were screened for the desired homologous recombination event by Southern blot analysis. Twelve ES cell clones harboring the desired homologous recombination were identified from a total of 192 analyzed colonies. Three clones were injected into C57BL/6 blastocysts, and all three clones gave rise to male chimeras that displayed germ-line transmission. These chimeras were mated with C57BL/6 females to generate heterozygous mutant mice. The resulting heterozygous mice were intercrossed to generate homozygous mutants.

To assess the disruption of the *m*-neu1 gene, we analyzed the *m*-neu1 genomic locus as well as the levels of *m*-neu1 mRNA. Analysis of genomic DNAs from F2 mice by Southern blotting with either a 5′-specific probe or a 3′-specific probe indicated that the 4.8-kb fragment in the *m*-neu1 genomic locus was indeed replaced by the neomycin resistance gene (Fig. 4*b*). PCR analysis of genomic DNAs further confirmed the disruption of the *m*-neu1 genomic locus (Fig. 4*c*). Northern blot analysis, with a probe to the 5′ *m*-neu1 cDNA, revealed the total absence of *m*-neu1 mRNAs in homozygous mutants (Fig. 4*d*). In addition, mRNA levels found in heterozygous mutants were about 50% of those found in wild-type mice (Fig. 4*d*). Taken together, these data suggest that *m*-neu1 gene is disrupted, resulting in a null mutation.

***m*-neu1$^{-/-}$ Mice Are Viable and Morphologically Normal.** The offspring of wild-type, heterozygous, and homozygous mutants from crosses of heterozygotes were produced at the predicted Mendalian frequency (1:2:1), and *m*-neu1$^{-/-}$ mice are indistinguishable from wild-type littermates at embryonic and postnatal stages. *m*-neu1$^{-/-}$ mice also reproduced without any apparent deficit in fertility, litter size, or litter survival. No decrease in lifespan was noted for *m*-neu1$^{-/-}$ mice. The brain of the homozygous mutant has normal size, weight, and gross appearance in embryos as well as in adult animals. Histological analysis of the *m*-neu1$^{-/-}$ brain, by hematoxylin and eosin staining and cresyl violet (Nissl) staining, revealed no detectable abnormality at different developmental stages (data not shown). Even in the

NEUROBIOLOGY

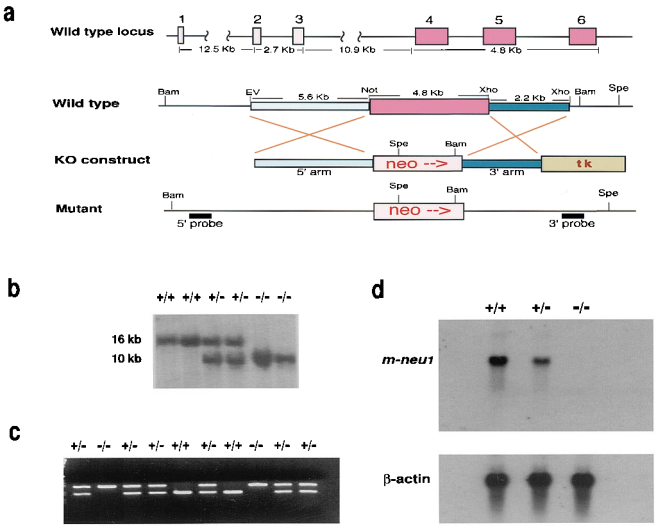

Fig. 4. Targeted disruption of the *m*-neu1 gene. (*a*) Schematic diagram of the targeting strategy, showing the organization of the wild-type *m*-neu1 genomic region, the targeting construct, and the mutant allele that results from homologous recombination of the targeting vector at the *m*-neu1 locus. Exons are shown as closed boxes; neo, neomycin-resistant gene cassette; tk, thymidine kinase gene cassette. The transcription orientation of neo cassette is shown by the arrow. The 5′ and 3′ probes that are external to the vector region are indicated at the bottom. (*b*) Southern blot analysis of *Bam*HI-digested DNAs from six littermates after hybridization with a 5′ probe. The wild-type allele yields a 16-kb band, and the mutant allele yields a 10-kb band. Genotypes are indicated above each lane: wild-type (+/+), heterozygous (+/−), and homozygous (−/−). (*c*) Genotype analysis by PCR. Three primers were used (see *Methods*). Primer 1 and primer 2 generate a 190-bp fragment that represents wild-type allele, whereas primer 2 and primer 3 produce a 270-bp fragment indicative of the knockout allele. (*d*) Detection of *m*-neu1 transcript by Northern blot analysis. Brain poly(A)$^+$ RNAs (2 μg) from wild-type (+/+), heterozygous (+/−), and homozygous (−/−) were blot-hybridized with a probe specific for *m*-neu1. A *β-actin* probe was used as a control.

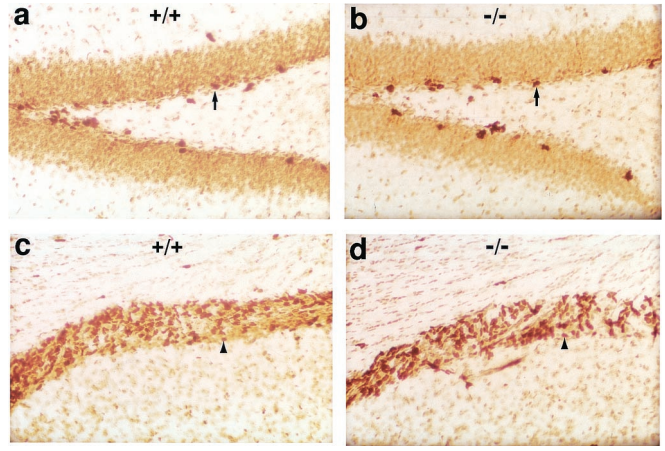

Fig. 5. Adult neurogenesis in the dentate gyrus and chain migration of neuronal precursors in the rostral migratory stream (RMS) are indistinguishable in wild-type mice and *m*-neu1$^{-/-}$ mice. BrdUrd-labeled neurons (arrow) in the dentate gyrus of wild-type mice (*a*) and *m*-neu1$^{-/-}$ mice (*b*). BrdUrd-labeled neuronal precursors (arrowhead) in the rostral migratory stream of wild-type (*c*) and *m*-neu1$^{-/-}$ mice (*d*).

regions where *m*-neu1 is highly expressed, such as the cerebral cortex, cerebellum, striatum, hippocampus, and dentate gyrus, no obvious morphological abnormalities were detected. Moreover, in the *m*-neu1$^{-/-}$ brain, adult neurogenesis in the dentate gyrus (30) and chain migration of neuronal precursors in the rostral migratory stream (31) are also indistinguishable from that in the wild-type littermate brain, as indicated by labeling with BrdUrd (Fig. 5). Furthermore, no differences were noted between *m*-neu1$^{-/-}$ mice derived from two other independently targeted ES recombinants.

***m*-neu1$^{-/-}$ Mice Exhibit a Defect in Olfactory Discrimination.** *m*-neu1 is widely expressed in differentiated neurons in the central nervous system. *m*-neu1 is also expressed in sensory neurons in the olfactory epithelium and in the vomeronasal organ. We speculated that *m*-neu1 may play a role in neuronal function in adult mice. Therefore, the behaviors of adult *m*-neu1$^{-/-}$ mice were evaluated by a battery of behavioral tests, including a rotarod assay for motor coordination (32), open field exploration (33), seizure induction by pentylenetetrazol or kainic acid (34), olfactory discrimination (23–25), pain sensation by hot-plate assay (35), aggression by resident-intruder assay (36), and maternal behavior by pup retrieval test (37). From these many tests, only the following behavioral abnormalities in *m*-neu1$^{-/-}$ mice were observed: *m*-neu1$^{-/-}$ mice exhibited an olfactory discrimination defect and *m*-neu1$^{-/-}$ mice were hypersensitive to ethanol effects on motor coordination (see below).

Olfactory discrimination is assessed by using a conditioned avoidance procedure in which exposure to an odorant in a drinking tube is associated with an aversive stimulus, LiCl injection (23–25). Animals subsequently avoid the test odorant when reexposed to the odorant at a later time. A two-bottle preference procedure was used to assess avoidance of odorant. Measurement of preference ratio (volume of odorant solution consumed/total solution consumed) as determined in this two-bottle preference assay has been shown to be an assessment of olfactory function rather than taste (23, 24). In this behavioral assay, no significant differences were observed in total fluid intake between wild-type mice and *m*-neu1$^{-/-}$ mice. However, significant differences ($P < 0.05$) were observed in preference ratio between wild-type mice ($n = 13$) and *m*-neu1$^{-/-}$ mice ($n = 16$) at 10^{-3} M, 10^{-4} M, and 10^{-5} M isovaleric acid concentrations (Fig. 6). The defect most likely reflects a reduced ability of the mutant mice to detect the odorant rather than a deficiency in associative learning because both *m*-neu1$^{-/-}$ mice and wild-type mice learned to avoid drinking fluid containing 10^{-3} M isovaleric acid that was associated with lithium injection, exhibiting a preference ratio equal to or less than 10%, respectively. To further assess the learning ability of *m*-neu1$^{-/-}$ mice, we examined their spatial learning and memory in Morris water maze

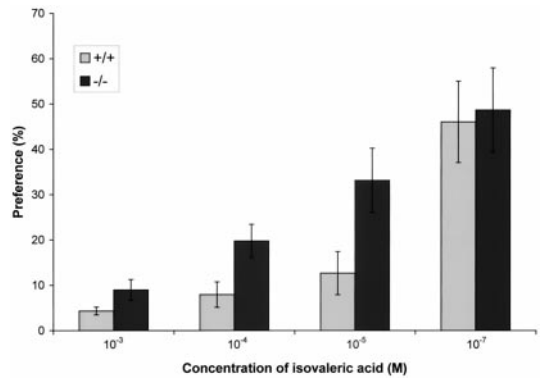

Fig. 6. *m*-neu1$^{-/-}$ mice are defective in olfactory discrimination. The preference (%) shown on the *y* axis is the percentage of isovaleric acid solution consumed of the total solution consumed. Values represent group means ± SD. Data analysis (one-way ANOVA) revealed the significant difference ($P < 0.05$) between wild-type ($n = 13$) and *m*-neu1$^{-/-}$ mice ($n = 16$) at the 10^{-3} M, 10^{-4} M, and 10^{-5} M isovaleric acid concentrations.

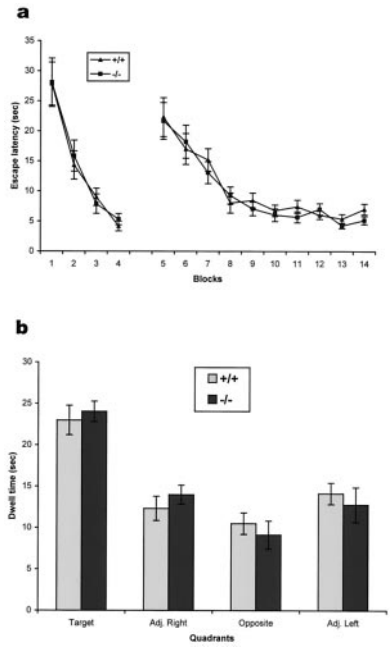

Fig. 7. *m*-neu1$^{-/-}$ mice exhibit normal learning and memory in the Morris water maze. (*a*) Escape latencies are comparable for the *m*-neu1$^{-/-}$ mice and wild-type mice in the acquisition phase. The time it took for the mouse to reach the platform was plotted for the visible-platform task in the first 2 days (blocks 1–4) and the hidden-platform task in the following 5 days (blocks 5–14). (*b*) Quadrant preferences of *m*-neu1$^{-/-}$ mice and wild-type mice in the probe test, which is just after the 7-day training and is in the absence of platform. The time spent in each quadrant during a 60-s probe test is plotted. There were no significant differences between *m*-neu1$^{-/-}$ mice and wild-type mice, indicating that *m*-neu1$^{-/-}$ mice have normal memory. All values are mean ± SEM.

(38). Like wild-type mice, these mutant mice learned to locate the visible platform and then the hidden platform (Fig. 7*a*). A probe test, in the absence of platform and just after the training, showed that both the *m*-neu1$^{-/-}$ and wild-type mice remembered equally well where the hidden platform used to be (Fig. 7*b*). These results reinforce the notion that *m*-neu1$^{-/-}$ mice have normal learning and memory. Their reduced ability to avoid the odorant isovaleric acid (Fig. 6) reflects their impaired olfactory discrimination.

***m*-neu1$^{-/-}$ Mice Are Hypersensitive to Ethanol Effects on Motor Coordination.** Ethanol effects on motor coordination were examined by using the rotarod assay. Performance of this task involves both the cerebellum and striatum, where the *m*-neu1 gene is highly expressed. Before ethanol injection, no significant difference was observed in the duration that wild-type mice and *m*-neu1$^{-/-}$ mice remained on rotarod (the latency to falling off). However, after ethanol injection (2.0 g/kg, i.p.), a significant difference ($P < 0.05$) was observed in such latencies on rotarod between wild-type mice ($n = 15$) and *m*-neu1$^{-/-}$ mice ($n = 16$) (Fig. 8). Thus, *m*-neu1$^{-/-}$ mice are hypersensitive to ethanol effects on motor coordination. Analysis of the blood ethanol concentration showed no difference between wild-type mice and *m*-neu1$^{-/-}$ mice. Because ethanol triggers widespread apoptotic neurodegeneration in developing brain (39), we examined ethanol-induced apoptotic neurodegeneration in *m*-neu1$^{-/-}$ mice and wild-type littermates and found no differences between these two genotypes. Moreover, we also found no differences in ethanol preference (40) between *m*-neu1$^{-/-}$ mice and wild-type littermates in a two-bottle preference test (data not shown), confirming that *m*-neu1$^{-/-}$ mice are hypersensitive to ethanol.

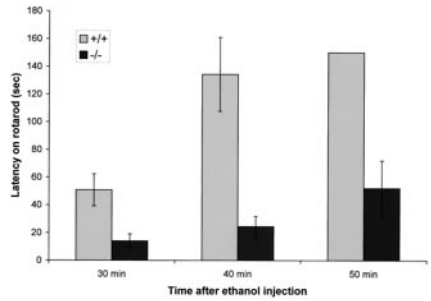

Fig. 8. *m*-neu1$^{-/-}$ mice are hypersensitive to the effect of ethanol on motor coordination. Wild-type and *m*-neu1$^{-/-}$ mice were injected with ethanol (2.0 g/kg, i.p.), and their performance on the rotarod was examined 30, 40, and 50 min after ethanol injection. By 50 min, all of the wild-type mice stayed on the rotarod longer than 150 s, and their latency was recorded as 150 s. Values represent group mean ± SD. Data analysis (one-way ANOVA) revealed the significant difference ($P < 0.05$) between wild-type ($n = 15$) and *m*-neu1$^{-/-}$ ($n = 16$) mice at each time point tested.

Discussion

We have reported here the cloning and characterization of a mouse gene, *m*-neu1, whose deduced amino acid sequence shows significant homology to the *Drosophila* Neuralized (D-Neu) protein. The sequence homology between M-Neu1 and D-Neu is present throughout the two proteins, including the highly conserved C3HC4 RING zinc finger domain that may mediate protein interaction (26). To determine whether the neural functions might be conserved between M-Neu1 and D-Neu, we first examined RNA expression pattern of *m*-neu1 gene during embryonic, postnatal, and adult stages. Our results show that *m*-neu1 is mainly expressed in the nervous system in E8.5 embryos. At later embryonic and postnatal stages, the *m*-neu1 transcript is expressed in differentiated neurons in the central nervous system as well as in sensory neurons of the olfactory epithelium and the vomeronasal organ. Thus, the expression pattern of *m*-neu1 suggests a potential functional role of *m*-neu1 in the nervous system.

We examined the *in vivo* function of *m*-neu1 by disrupting the *m*-neu1 gene through homologous recombination in mouse embryonic stem cells. Mice homozygous for the *m*-neu1 disruption are viable and morphologically normal. Two possibilities could explain the lack of readily detectable phenotypes affecting nervous system formation. The first possibility is that *m*-neu1 is not involved in this process, even though *d-neu* is required for neurogenesis and null mutation of *d-neu* results in embryonic lethality in *Drosophila*. An alternative possibility, which we favor, is that *m*-neu1 is involved in nervous system formation but that its loss in *m*-neu1$^{-/-}$ mutants is functionally compensated for by the existence of other mouse *neuralized* homolog(s). Functional compensation or redundancy is likely to account for the mutant phenotypes in mice and other organisms. Indeed, there is a second mouse homolog of *Drosophila neuralized* (*m*-neu2), whose expression overlaps with, but is broader than, that of *m*-neu1 (Y.R. and Y.N.J., unpublished results). The question of possible functional redundancy between the two mouse homologs may be answered by future studies of the phenotypes of *m*-neu2 mutants and *m*-neu1/*m*-neu2 double mutants.

We found that *m*-neu1$^{-/-}$ mice displayed an olfactory discrimination defect and that *m*-neu1$^{-/-}$ mice were more sensitive to the effect of ethanol on motor coordination. These results indicate that *m*-neu1 is important for the proper formation and/or function of the nervous system structures critical for these behaviors. Loss of one of the two *m*-neu genes identified thus far, *m*-neu1, may result in developmental defects too subtle to be readily detected by routine histological procedures and

light microscopy. In addition, *m*-neu1 may function in the adult nervous system. It is conceivable that M-Neu1 may participate in signal transduction in the adult nervous system. The behavioral defects uncovered in this study identify the circuitry for olfactory processing and the circuitry for motor coordination and ethanol sensitivity as brain regions that critically depend on *m*-neu1 gene activity for their proper function.

The *m*-neu1 gene is expressed in the olfactory epithelium, olfactory cortex, and olfactory bulb. The olfactory discrimination assay we used has been shown to assess olfactory function rather than taste (23, 24). The *m*-neu1$^{-/-}$ mice exhibited normal spatial learning and memory in the Morris water maze (Fig. 7) and hence are likely to possess the faculty to associate the odorant with the unpleasant reaction to lithium in the same fluid. The poor performance of *m*-neu1$^{-/-}$ mice in the olfactory discrimination test probably reflects their impaired ability to detect the odorant rather than a learning defect because at the highest odorant concentrations tested, the mutant mice clearly showed avoidance of the fluid they drank shortly after the averse lithium treatment (Fig. 6), indicating that they are capable of this form of associative learning of profound importance to survival. Compared with their wild-type littermates, however, they required roughly 10-fold higher concentration of the odorant to elicit roughly the same level of avoidance, indicating that the *m*-neu1$^{-/-}$ mice have a specific lesion in olfactory processing. The *m*-neu1 gene is also expressed in cerebellum and striatum. These two regions are related to motor coordination. Although *m*-neu1$^{-/-}$ mice did not exhibit an obvious defect in motor coordination before ethanol injection, *m*-neu1$^{-/-}$ mice are hypersensitive to acute access to ethanol on motor coordination, indicating that *m*-neu1 is involved in behavioral response to ethanol. Ethanol exerts various detrimental behavioral effects in humans, but the underlying neuronal mechanisms are still not understood.

In summary, we have identified functional requirements of *m*-neu1 in olfactory discrimination and ethanol effects on motor coordination by targeting *m*-neu1 gene and using expression pattern as guidance to design behavioral tests. These results suggest that mammalian *neuralized*, like mammalian *Notch*, may be involved throughout the life of neurons, playing a role not only at a neuron's birth but also in adult stage. Furthermore, these findings provide leads to future studies on the molecular mechanisms of ethanol effects and olfactory processing.

We are very grateful to members of the Jan laboratory for discussion, suggestions, and help. We thank Drs. Stephen J. Bonasera and Hung-Ming Chu for help in behavioral tests, and Juanito J. Meneses and Dr. Roger A. Pedersen for help in gene targeting. We also thank Drs. Yee-Ming Chan and Bingwei Lu for critical reading of the manuscript. This work was supported by a National Institute of Mental Health grant to the Silvio Conte Center for Neuroscience Research at University of California, San Francisco. Y.R. was supported by the Biomedical Science Program at University of California, San Francisco. L.T. was supported by National Institute of Mental Health K02 Award MH01949. L.Y.J. and Y.N.J. are investigators of the Howard Hughes Medical Institute.

1. Lewis, J. (1996) *Curr. Opin. Neurobiol*. **6,** 3–10.
2. Anderson, D. J. & Jan, Y. N. (1997) in *Molecular and Cellular Approaches to Neural Development*, eds. Cowan, W. M., Jessell, T. M. & Zipursky, S. L. (Oxford Univ. Press), pp. 26–63.
3. Chan, Y. M. & Jan, Y. N. (1999) *Curr. Opin. Neurobiol.* **9,** 582–588.
4. Artavanis-Tsakonas, S., Matsuno, K. & Fortini, M. (1995) *Science* **268,** 225–232.
5. Robby, E. (1997) *Curr. Opin. Genet. Dev.* **7,** 551–557.
6. Selkoe, D. J. (2000) *Curr. Opin. Neurobiol.* **10,** 50–57.
7. Giniger, E. (1998) *Neuron* **20,** 667–681.
8. Giniger, E., Jan, L. Y. & Jan, Y. N. (1993) *Development (Cambridge, U.K.)* **117,** 431–440.
9. Sestan, N., Artavanis-Tsakonas, S. & Rakic, P. (1999) *Science* **286,** 741–746.
10. Redmond, L., Oh, S. R., Hicks, C., Weinmaster, G. & Ghosh, A. (2000) *Nat. Neurosci.* **3,** 30–40.
11. Lehmann, R., Jimenez, F., Dietrich, U. & Campos-Ortega, J. A. (1983) *Wilhelm Roux's Arch. Dev. Biol.* **192,** 62–74.
12. Campos-Ortega, J. A. (1988) *Trends Neurosci.* **11,** 400–405.
13. Boulianne, G. L., de la Concha, A., Campos-Ortega, J. A., Jan, L. Y. & Jan, Y. N. (1991) *EMBO J.* **10,** 2975–2983.
14. Price, B. D., Chang, Z., Smith, R., Bockheim, S. & Laughon, A. (1993) *EMBO J.* **12,** 2411–2418.
15. Yeh, E., Zhou, L., Rudzik, N. & Boulianne, G. L. (2000) *EMBO J.* **19,** 4827–4837.
16. Lai, E. C. & Rubin, G. M. (2001) *Dev. Biol.* **231,** 217–233.
17. Lai, E. C. & Rubin, G. M. (2001) *Proc. Natl. Acad. Sci. USA* **98,** 5637–5642.
18. de la Concha, A., Dietrich, U., Weigel, D. & Campos-Ortega, J. A. (1988) *Genetics* **118,** 499–508.
19. Saurin, A. J., Borden, K. L. B., Boddy, M. N. & Freemont, P. S. (1996) *Trends Biochem. Sci.* **21,** 208–214.
20. Church, G. M. & Gilbert, W. (1984) *Proc. Natl. Acad. Sci. USA* **81,** 1991–1995.
21. Wilkinson, D. G. (1992) in *In Situ Hybridization: A Practical Approach*, ed. Wilkinson, D. G. (IRL Press, Oxford), pp. 75–83.
22. Schaeren-Wiemers, N. & Gerfin-Moser, A. (1993) *Histochemistry* **100,** 431–440.
23. Wysocki, C. J., Whitney, G. & Tucker, D. (1977) *Behav. Genet.* **7,** 171–188.
24. Pourtier, L. & Sicard, G. (1989) *Behav. Genet.* **20,** 449–509.
25. Griff, I. C. & Reed, R. R. (1995) *Cell* **83,** 407–414.
26. Borden, K. L. B. & Freemont, P. S. (1996) *Curr. Opin. Struct. Biol.* **6,** 395–401.
27. Nakamura, H., Yoshida, M., Tsuiki, H., Ito, K., Ueno, M., Nakao, M., Oka, K., Tada, M., Kochi, M., Kuratsu, J., *et al.* (1998) *Oncogene* **16,** 1009–1019.
28. Mansour, S. L., Thomas, K. R. & Capecchi, M. R (1988) *Nature (London)* **336,** 348–352.
29. Nagy, A., Rossant, J., Nagy, R., Abramow-Newerly, W. & Roder, J. C. (1993) *Proc. Natl. Acad. Sci. USA* **90,** 8424–8428.
30. Kempermann, G., Kuhn, H. G. & Gage, F. H. (1997) *Nature (London)* **386,** 493–495.
31. Lois, C., Garcia-Verdugo, J. M. & Alvarez-Buylla, A. (1996) *Science* **271,** 978–981.
32. Jones, B. J. & Roberts, D. J. (1968) *Naunyn-Schmiedeberg's Arch. Pharmacol.* **259,** 211.
33. Dishman, R. K., Armstrong, R. B., Delp, M. D., Graham, R. E. & Dunn, A. L. (1988) *Physiol. Behav.* **43,** 541–546.
34. Kosobud, A. E. & Crabbe, J. C. (1990) *Brain Res.* **526,** 8–16.
35. Pick, C. G., Cheng, J., Paul, D. & Pasternak, G. W. (1991) *Brain Res.* **566,** 295–298.
36. Nelson, R. J., Demas, G. E., Huang, P. L., Fishman, M. C., Dawson, V. L., Dawson, T. M. & Synder, S. H. (1995) *Nature (London)* **378,** 383–386.
37. Nishimori, K., Young, L. J., Guo, Q., Wang, Z., Insel, T. R. & Matzuk, M. M. (1996) *Proc. Natl. Acad. Sci. USA* **93,** 11699–11704.
38. Morris, R. G., Garrud, P., Rawlins, J. N. & O'Keefe, J. (1982) *Nature (London)* **24,** 681–683.
39. Ikonomidou, C., Bittigau, P., Ishimaru, M. J., Wozniak, D. F., Koch, C., Genz, K., Price, M. T., Stefovska, V., Horster, F., Tenkova, T., *et al.* (2000) *Science* **287,** 1056–1060.
40. Phillips, T. J., Brown, K. J., Burkhart-Kasch, S., Wenger, C. D., Kelly, M. A., Rubinstein, M., Grandy, D. K. & Low, M. J. (1998) *Nat. Neurosci.* **1,** 610–615.